

Comparative performance of RC shear walls designed by different standards

*Farhad Dashti¹⁾ and Rajesh P Dhaka²⁾

^{1), 2)} *Department of Civil and Natural Resources Engineering, University of Canterbury, Private Bag 4800, Christchurch 8140, New Zealand,*

¹⁾ *farhad.dashti@pg.canterbury.ac.nz*

ABSTRACT

Structural walls (also known as shear walls) are one of the common lateral load resisting elements in reinforced concrete (RC) buildings in seismic regions. The performance of RC structural walls in recent earthquakes has exposed some problems with the existing design of RC structural walls. The main issues lie around the buckling of bars, out-of plane deformation of the wall (especially the zone deteriorated in compression), reinforcement getting snapped beneath a solitary thin crack etc. This study compares design provisions of detailing requirements of RC shear walls provided by different design codes by evaluating performance of a typical wall designed by different standards. For this purpose, a case study RC shear wall is taken from the Hotel Grand Chancellor in Christchurch which was designed according to the 1982 version of the New Zealand concrete structures standard (NZS3101:1982). The wall is redesigned in this study to comply with the detailing requirements of three standards; ACI-318-11, NZS3101:2006 and Eurocode 8 in such a way that they provide the same flexural and shear capacity. Based on section analysis and pushover analysis, nonlinear responses of the walls are compared in terms of their lateral load capacity and curvature as well as displacement ductilities, and the effect of the code limitations on nonlinear responses of the different walls are evaluated. A parametric study is also carried out to further investigate the effect of confinement length on the lateral response of shear walls.

Keywords: Reinforced concrete; Shear wall; Design codes; Comparative performance; Confinement length

1. INTRODUCTION

The structural wall system was introduced in the 1970s, and design provisions for this system have evolved since then. Barbell-shaped wall sections with boundary elements protruding from the surface of the wall were more common in the 1970s and 1980s. In this system, the boundary elements acted as columns resisting axial load and

overturning. In recent years, as the optimization issues have gained importance, slender rectangular walls which take less space and are behaved to be more economical designs have become more common in many countries like New Zealand. Use of higher concrete strengths has also resulted in more slender profiles than have been previously tested in the laboratory or in real buildings under earthquakes. Slender walls with nominal reinforcing and higher axial load have failed in recent earthquakes in brittle shear-compression mode or by premature fracture of tensile/compressive reinforcing bars (Wallace 2012).

The RC buildings in New Zealand can be classified into two categories; namely Pre-1970 buildings which were designed prior to the 1976 revision of the RC seismic design code NZS4203:1976, and modern buildings that were designed using the 1976 or a later version of the RC seismic design code. Pre-1970s RC buildings generally have inadequate seismic capacity and are likely to experience brittle failure as they have deficiencies like lack of confinement in walls, joints and columns, inadequate reinforcing and anchorage details, poor material properties and use of plain reinforcing bars, no capacity design principles and irregular building configurations (Kam et al. 2011). According to the EERI special earthquake report on the M6.3 Christchurch, New Zealand, earthquake of February 22 (2011) and Canterbury Earthquakes Royal Commission Reports (2012), structural walls did not perform as anticipated. Boundary zone crushing and bar buckling were observed mostly in Pre-1970s RC walls which were generally lightly reinforced, were not detailed for ductility and had inadequate reinforcement to provide confinement to the concrete and buckling restraint to the longitudinal reinforcement.

On the other hand, modern (Post-1970s) RC wall buildings were observed to have experienced failure patterns like wall web buckling, boundary zone bar fracture and buckling failure of ducted splice. In a number of cases, compression failure occurred in the outstanding legs of T and L walls in addition to significant out-of-plane displacements, thereby resulting in overall buckling of the wall. In some cases, the transverse reinforcement did not meet the spacing requirement to prevent buckling of the longitudinal reinforcement, and bar buckling resulted in high localized strains and decreased the tensile strain capacity. Figure 1 and Figure 2 show some examples of different failure modes, observed in RC walls in 2011 Christchurch earthquake.

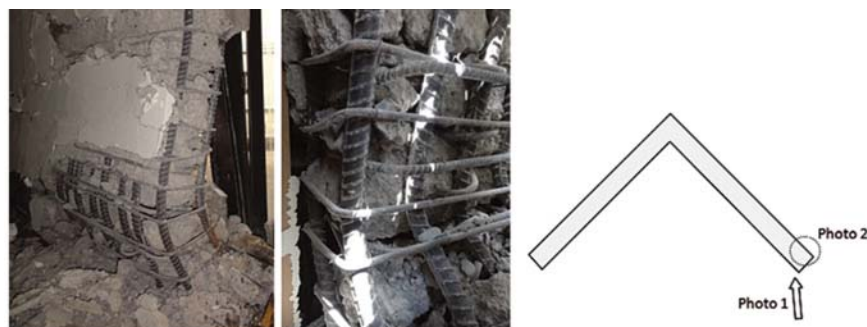


Figure 1. Web buckling of well-confined wall (Elwood 2013)



**Figure 2: a) Bar buckling and fracture in lightly reinforced slender RC shear wall
b) Slender wall shear-axial failure (Kam et al. 2011)**

As a result of the performance of the shear walls in recent earthquakes in New Zealand, some issues have been identified to be further investigated (NZRC 2012). The reinforcement ratio and arrangement turned out to be inadequate in some of the damaged walls and resulted in formation of a single primary crack. The reinforcement ratio should ensure extended yielding beyond the vicinity of a single crack. This issue can be sorted out by using higher minimum reinforcement ratio, changing distribution of the reinforcement and de-bonding bars in the critical zones (NZRC 2012). Also, there are some issues that considerably affected the performance of structural walls in buildings. For instance, some walls sustained greater axial forces than were anticipated in the design due to the fact that as reinforcement yielding and formation of plastic hinge started in the wall, other structural elements provided restraint against elongation of the wall and resulted in considerable increase in the axial load ratio.

Compression yielding of the vertical reinforcement in unconfined region of the wall can result in buckling. In other words, if the provided confinement length is not enough to cover the whole compression area of the wall where axial compressive strain can be considerably beyond the yield point of steel and crushing strain of concrete, vertical reinforcement of the unconfined zone may undergo big strains and cause sudden degradation in overall response of the wall.

The effect of bi-directional loading on walls has received little attention from researchers, and most wall experiment results used to establish design provisions tested response of the walls under in-plane loading only. In some damaged walls like the one in the Christchurch Grand Chancellor Hotel building, out of plane failure of the wall at the base was observed, which could have been triggered by ground motions in the out of plane direction.

Another issue that became a matter of concern in recent earthquakes in New Zealand (2011) and also in Chile (2010) was the slenderness ratio of walls for which suitable provisions are not provided in design codes to prevent buckling of walls subjected to moderate and high axial load ratios (Telleen et al. 2012).

In this study, detailing requirements of reinforced concrete shear walls provided by different design codes are compared by designing a typical wall based on different standards and evaluating their performance. For this purpose, one of the RC shear

walls damaged in the 2011 Christchurch earthquake was used for comparison. The wall is taken from the Christchurch Grand Chancellor Hotel which was severely damaged (requiring demolition) in the 22 February 2011 earthquake.

2. COMPARATIVE DESIGN:

2.1 Case study wall

The Hotel Grand Chancellor was one of the severely damaged buildings during the 22 February 2011 Christchurch earthquake. The tower was constructed between 1985 and 1988 according to the NZS4203:1984 loading standard and NZS3101:1982 concrete design standard, and was the tallest building in Christchurch at the time of construction. As shown in Figure 3, the lateral load resisting system comprised of RC shear walls in the lower tower and moment-resisting RC frames in the upper tower resulting in the vertical irregularity of the structure (DunningThorntonReport 2011). The building has horizontal irregularity as well, arising from the cantilever bay between grids D and E. The east side of the building (bay D-E) was cantilevered over an adjacent service lane (

Figure 3). Several deep transfer girders were used between levels 12 and 14 to transfer the cantilever load to the adjacent lane leading to a considerably great amount of axial load applied to a critical shear wall denoted as D5-6 in

Figure 3. Wall D10-11 was almost under the same loading condition but was completely different from Wall D5-6 in terms of reinforcement arrangement and maximum story height (3.6 m, compared to 5.1 m for wall D5-6) and had a return wall at one end to help support the high axial loads. As shown in

Figure 4, wall D5-6 suffered a brittle failure at the base with out-of-plane instability. The failure plane initiated at the top of the lap splice in the web vertical reinforcement. The confinement hoops opened allowing the longitudinal bars to deform with the shortening of the wall. This wall was subjected to excessive amount of axial load from the cantilever structure, the corner column of the upper tower perimeter moment frame and the vertical excitation of the cantilever structures both above and below level 14. The combined axial load and bending exceeded the concrete compression strain capacity given the limited tie reinforcement provided at the base of the wall. Some out-of-plane drift of the wall during the earthquake excitation and the plane of weakness created at the end of the splice of the web vertical reinforcement further contributed to the failure at its base. Figure 5 displays the reinforcement configuration of the wall along the length and height of the wall. Scrutinizing these details indicates a deficient confinement length and inadequate reinforcement ratio in the boundary element.

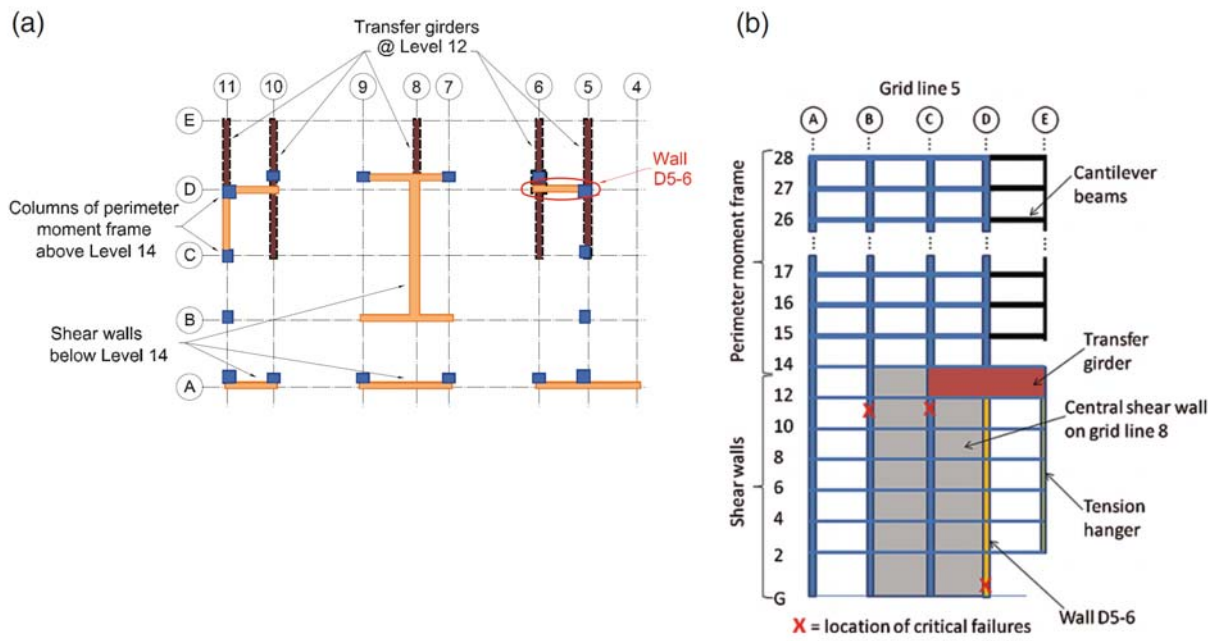


Figure 3. Hotel Grand Chancellor structural layout sketch (a) plan; (b) elevation along grid line 5 (Elwood 2013)



Figure 4. Failure of Shear wall D5-6

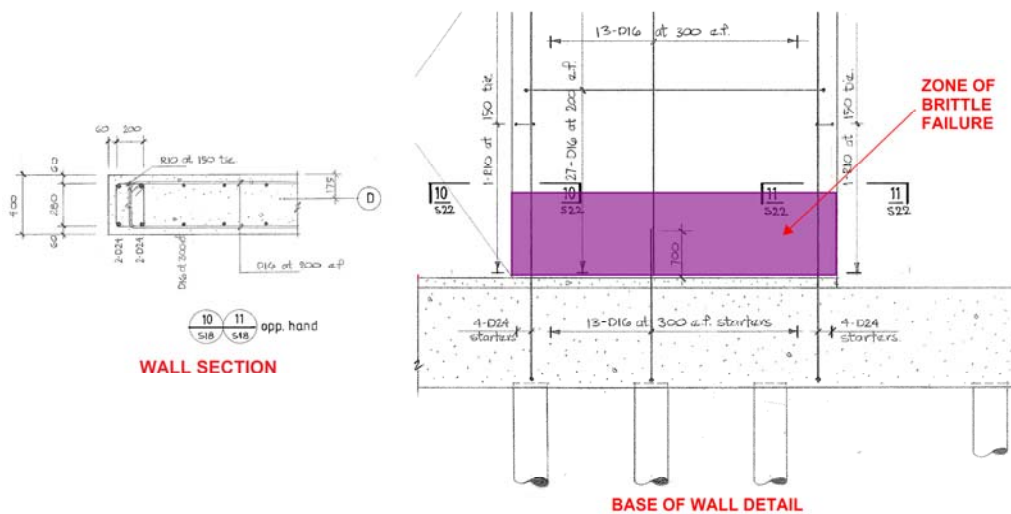


Figure 5. Reinforcement details of wall D5-6 (DunningThorntonReport 2011)

2.2 Modified Design

According to a consultancy report investigating into the performance of this wall (DunningThorntonReport 2011), the original design actions of the wall are:

Axial Load = 17MN ($0.25 f_c A_g$)

Moment = 8MN

Shear = 800kN

The wall is redesigned in this study to comply with the detailing requirements of three standards: ACI-318-11 (2011), NZS3101:2006 (2006) and Eurocode 8 (CEN 2004) in such a way that the demand used for design of the as-built wall (Wall D5-6) could be met. Figure 6 displays the wall sections designed based on the three codes in comparison with the as-built section. The as-built wall section was modified to meet the design requirements of each code with the least possible changes.

Since ACI318-11 does not limit the web and boundary thickness of walls, the wall thickness was not changed. It should be noted that this issue is currently a matter of concern following the wall instabilities observed in Chile (2010) earthquake as the building code adopted in Chile in 1996 was based on ACI 318-95, except that the boundary element confinement was not required. According to ACI318-11 Equation (21-8), special boundary elements are required for the wall with the minimum horizontal dimension calculated based on the neutral axis depth. The minimum length of confinement was calculated as 1365 mm which is considerably bigger than the 260 mm confinement length of the as-built wall. The confinement reinforcement of the as-built wall did not meet the minimum requirements of ACI318-11§ 21.9.6, and bigger size hoops with smaller spacing were used to satisfy the minimum allowable cross-section area of transverse reinforcement.

According to Eurocode 8, the minimum web thickness is governed by the story height and the minimum boundary thickness is calculated based on the confined length as well as the story height. The existing web thickness of the as-built wall was satisfactory and the confinement length was calculated based on the neutral axis position as well as the required value of the curvature ductility. Since the flexural

capacity of the wall was much greater than the flexural demand, the required curvature ductility was reduced resulting in a much smaller value for the confinement length than the ACI318-11 wall section. It should be noted that a bigger value for confinement length required a considerable increase in the minimum boundary element thickness (from 340 mm to 510 mm) and would cause a significant change in the wall section when compared to the sections designed by other codes as well as the as-built wall. Therefore, the minimum confinement length was adopted. The minimum volumetric ratio of confining reinforcement was satisfied using bigger hoop size with smaller spacing. Also, the maximum spacing of the longitudinal reinforcement was limited to 250 mm with cross-ties at every 500 mm connecting two curtains of reinforcement.

Different failure patterns including wall buckling under high axial load, flexural torsional buckling and out-of-plane buckling of the compression zone are addressed in the provisions of NZS3101:2006 for the minimum web and boundary thickness and the effective height to thickness ratio. The as-built wall satisfied the dimensional limitations but did not meet the confinement requirements in plastic hinge region and the modifications were made according to Section 11.4.6.5 of NZS3101:2006.

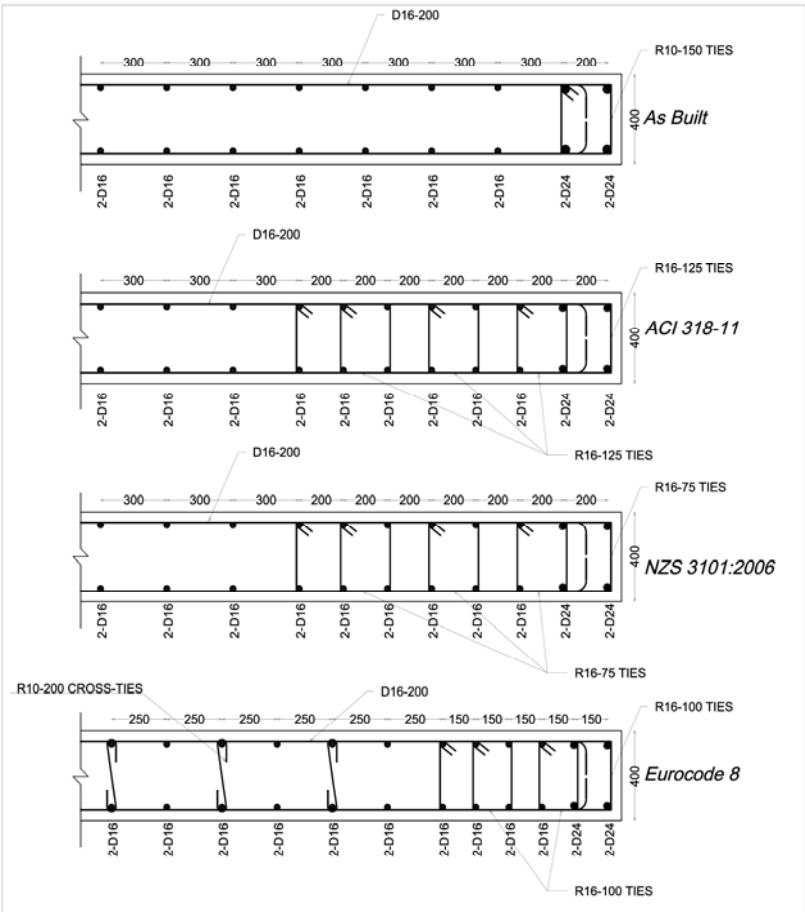


Figure 6. Wall sections

3. COMPARATIVE ANALYSIS

Nonlinear responses of the four wall models are compared in this section. First, section analysis is carried out to generate the moment-curvature response for each section. Then, the walls are modeled and analyzed in a FEM program to obtain their push-over curves.

3.1 Section Analysis

The major difference between the four wall sections is in the amount and arrangement of transverse hoops because of the different confinement requirements of the design standards. The axial stress-strain curves of the confined concrete obtained using Popovics/Mander's constitutive model (Mander et al. 1988) for the wall sections are compared in b)

Figure 7 (a). The ultimate strain of confined concrete is defined using the equation proposed by Priestley (1996). The stress-strain curve of the as-built configuration is considerably different from the curves of the other sections in terms of both strength and ductility and its ultimate strain is less than half of the strain capacity of the other sections. Figure 7 (b) shows the nonlinear stress-strain curve used for the reinforcing steel.

The moment-curvature curves of the wall sections generated using Xtract (TRC 2011) are shown in Figure 8 which clearly display the substantial deficiency of the as-built wall in terms of curvature ductility. As expected, the NZS3101 and ACI318 sections with better confinement (the larger amount of hoops and smaller spacing) sustained larger curvature before failure. The curvature ductility of the Eurocode8 section is higher than the as-built section but substantially less than the NZS3101 and ACI318 sections which is mainly due to its smaller confinement length when compared to the ACI318 and NZS3101 sections. It should be noted that, as shown in b)

Figure 7(a), the axial stress-strain curve of the confined concrete of the Eurocode8 section (originating from the size and spacing of hoops) indicates a confinement level that is as good as the ACI318 and NZS3101 sections, despite this, the moment-curvature curves of the three wall sections (Figure 8) are considerably different in terms of curvature ductility; this is mainly due to the difference in the confinement length which has a telling effect on the section behavior.

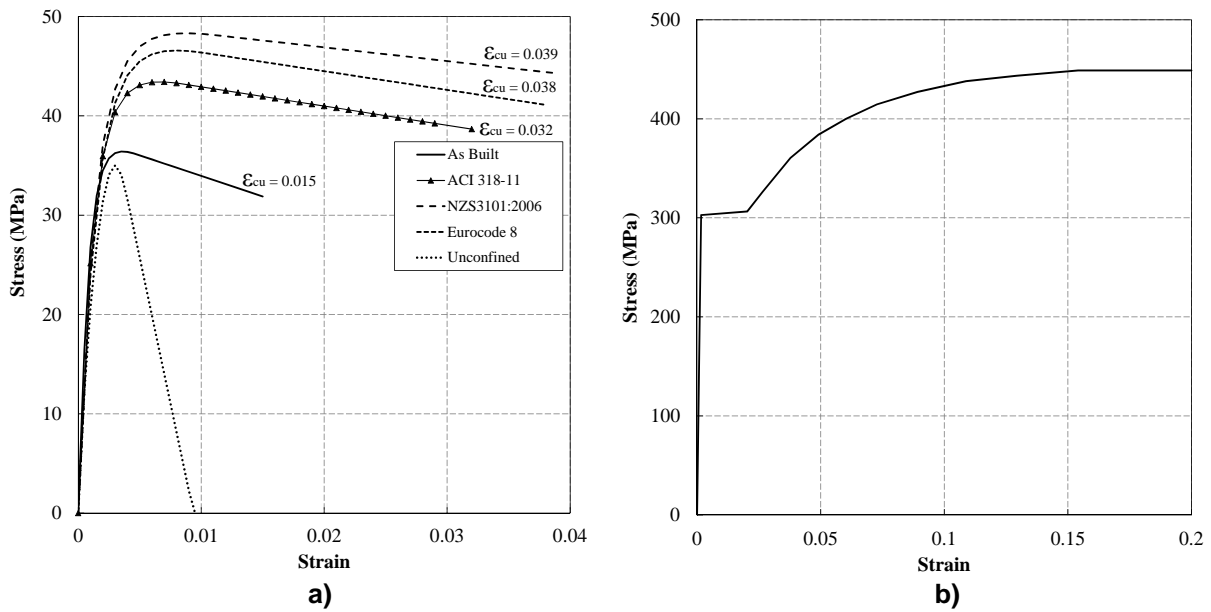


Figure 7: a) Confined concrete models of the wall sections
b) Stree-strain curve of the reinforcing steel

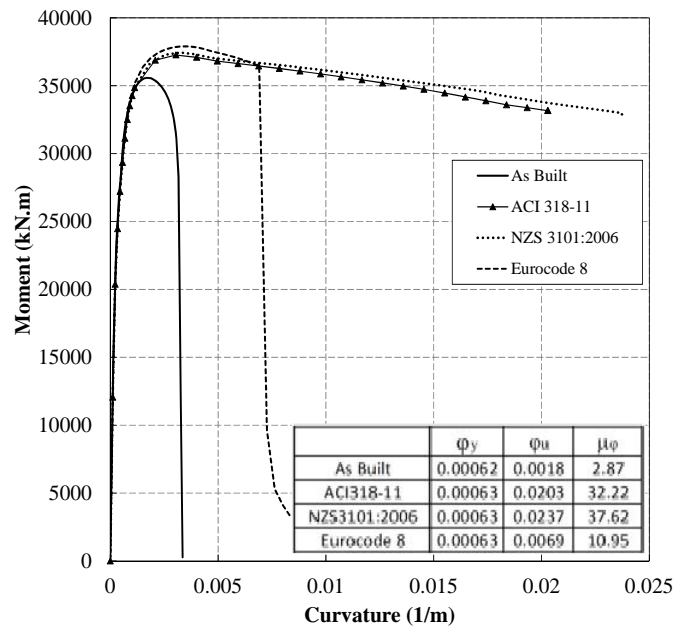


Figure 8. Moment-curvature curves of the wall sections

3.2 Push-over analysis

In order to capture the push-over curve of the wall sections, the walls were modeled in DIANA9.4.4 (DIANA 2011). Curved shell elements with embedded bar elements were used to simulate the reinforced concrete section. Out-of plane support was

provided at the story levels and a simplified displacement-controlled analysis was carried out with an incremental displacement applied at the top of the wall. The axial stress-strain data captured using Popovics/Mander's constitutive model (Mander et al. 1988) was implemented in the Total Strain Rotating Crack model (DIANA 2011) to incorporate the confined concrete properties in the boundary elements and behavior of the unconfined portion was modeled using the axial stress-strain relationship of unconfined concrete. The stress-strain curve of the reinforcing steel had a linear branch before yielding followed by a nonlinear hardening region (Figure 7(b)) after yielding using Von Mises Plasticity model available in DIANA.

Figure 9 displays the base shear versus top displacement response of the four walls. As shown in this figure, the as-built wall undergoes a brittle failure when the top displacement is only about 430 mm (i.e. 1.2% average drift). Failure of the Eurocode8 model was also accompanied by sudden degradation of the push-over curve, but the failure displacement was greater than twice of the as-built model. The models designed based on ACI318-11 and NZS3101:2006 were both ductile enough not to fail within the range of the analyzed displacement (i.e. 2000 mm top displacement or 5.5% average drift). It should be mentioned that reinforcement buckling and bond-slip failure were not considered in these models, although geometric nonlinearity was activated in the analysis to take the P-delta effect into account.

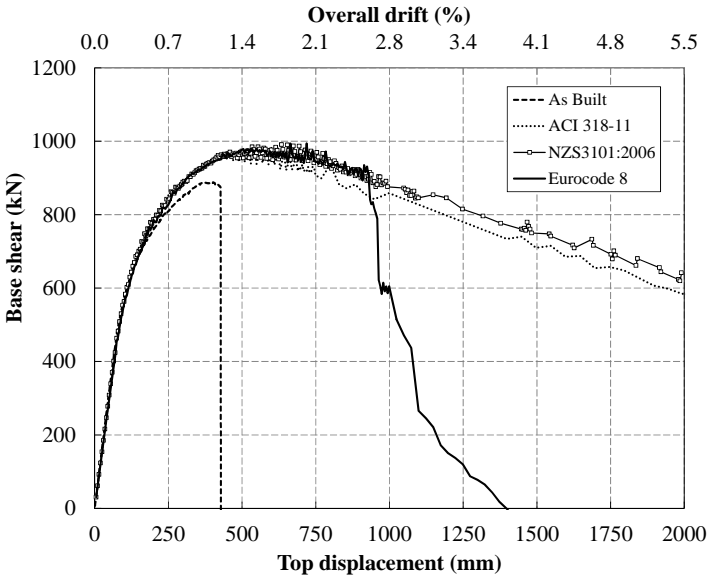


Figure 9. Base shear-top displacement response of the models

In order to scrutinize the nonlinear response of the wall models at different stages of displacement history, strain profiles along the wall sections as well as the inter-story drift profiles are plotted at some selected points corresponding to considerable changes in the slope of the push-over curves (Figure 10 to

Figure 13). These key points in the wall response correspond to cracking, yielding of tension and compression reinforcement and the ultimate point. The axial strain profile clearly shows the neutral axis position (corresponding to zero strain) at each stage. The confinement boundary is displayed in each graph to show the neutral axis position with regard to the boundary beyond which the concrete properties change from unconfined to confined or vice versa. Distribution of the reinforcement plastic strain along the length and along the height of the first story wall is displayed in Figure 14 to Figure 16. These figures display only the reinforcement strains and the dark shaded area shows the yielded reinforcement elements.

As shown in

Figure 10, at Point A, which corresponds to considerable cracking in the tension side of the wall, the neutral axis position is quite far from the extreme compression fiber which is obviously due to the substantially large axial load ($0.25 f_c A_g$). Yielding of the reinforcement at extreme compression and tension fibers start at Points B and C, respectively, resulting in considerable change of the neutral axis position. The axial load applied to the wall was so great that compression reinforcement yielded before the tension reinforcement. As the axial strain of the unconfined concrete exceeds the strain at the peak stress, strength degrades considerably in sufficient number of concrete elements, which results in overall collapse of the wall. In DIANA, the response of the embedded reinforcement is completely dependent on the mother element which is concrete in this case, and as the mother element becomes unstable, the whole element collapses. Figure 14 shows the plastic strain of the 1st story reinforcement of the as-built model. At Point D, where the ultimate capacity of the wall is reached, the number of yielded reinforcement is relatively small since the section was not ductile enough to allow much more uniform yielding along the wall length. The maximum plastic compressive strain of the reinforcement was 0.00365 at Point D which abruptly increased to 0.329 as the overall failure was observed (Figure 14). As shown in Figure 10, the as-built model could reach the displacement ductility of 1.4 and curvature ductility of 2.01, which is in agreement with the moment-curvature curve plotted in Figure 8. The inter-story drift profile of the wall also shows the incapability of the wall to reach an acceptable value of drift.

Figure 11 indicates the response of the wall designed based on ACI318-11. As previously mentioned, the wall did not fail even at a displacement equivalent to a drift value of 5.5% as the effect of reinforcement buckling and bond-slip was not taken into account. As a consequence, the point corresponding to 80% of the maximum strength of the wall was defined as the ultimate point (Point D). The axial strain versus wall length curve at different points, shown in

Figure 11, displays significant migration of the neutral axis position. Strain profiles corresponding to Points A to C are magnified in the figure to show the neutral axis position at these points. As shown in

Figure 11, the strain values of the ultimate point (Point D) are considerably bigger than the yield point (Point C). In this model the confinement was long enough to protect the unconfined concrete from reaching the peak strength. As shown in

Figure 11, the neutral axis was positioned within the confined concrete zone at the ultimate stage (Point D), where the confinement provided by the transverse reinforcement is enough to ensure a curvature ductility of 17.5 which corresponds to a

displacement ductility of 3.9. It should be noted that the ultimate strain of this model at the extreme compression element (0.04152) exceeds the ultimate strain value calculated for the confined concrete (0.032). However, the average strain of the mesh element equals 0.03298 which is consistent with the calculated value. Also, the ultimate curvature value (0.014 1/m) was calculated based on the sum of the extreme tension and compression strains divided by the whole length of the wall assuming a linear strain profile and is less than the value captured by the section analysis (Figure 8), whereas the curvature angle shown in

Figure 11 displays the effect of nonlinear strain profile on the value of curvature ductility. The distribution of reinforcement yielding in Figure 15 indicates capability of the wall to provide enough ductility and allow formation of a desirable plastic hinge at Point D. The reinforcement plastic strain at the top displacement of 1950 mm (5% drift) shows the fact that the increase rate in compression and tension strain was approximately identical and there was not a considerable change in neutral axis position. The inter-story drift profile of this model also shows its capability to reach a reasonable value of drift at the ultimate point.

The base shear versus top displacement response of the wall designed based on Eurocode8 shows considerable strength degradation at an average drift of 2.6% (Figure 12). According to the axial strain profile along the wall length, the confinement was not long enough to prevent the unconfined concrete from reaching the peak stress at the ultimate state. The calculated ductility values are 2.9 and 9.6 in terms of displacement and curvature, respectively. Also the value of ultimate curvature (0.0077 1/m) is in good agreement with the value obtained from the moment-curvature curve (Figure 8). The plastic strain distribution of the reinforcement within the 1st story (Figure 16) shows a considerable increase in compression strain with only 5mm increase of the wall top displacement which indicates a considerable shift of the neutral axis position resulting from failure of the compression concrete elements. According to Figure 13, response of the wall designed based on NZS3101:2006 showed a similar trend to the ACI318-11 model. The curvature and displacement ductility values were about 19 and 4.5, respectively, and the wall top displacement at failure (defined as 20% drop in strength) was about 1400 mm, which corresponded to an average drift of about 3.9%. As the strain profile of the NZS3101 wall along the length and across the height are quantitatively similar to the ACI318-11 model, the strain profiles are not separately illustrated for the NZS3101 wall.

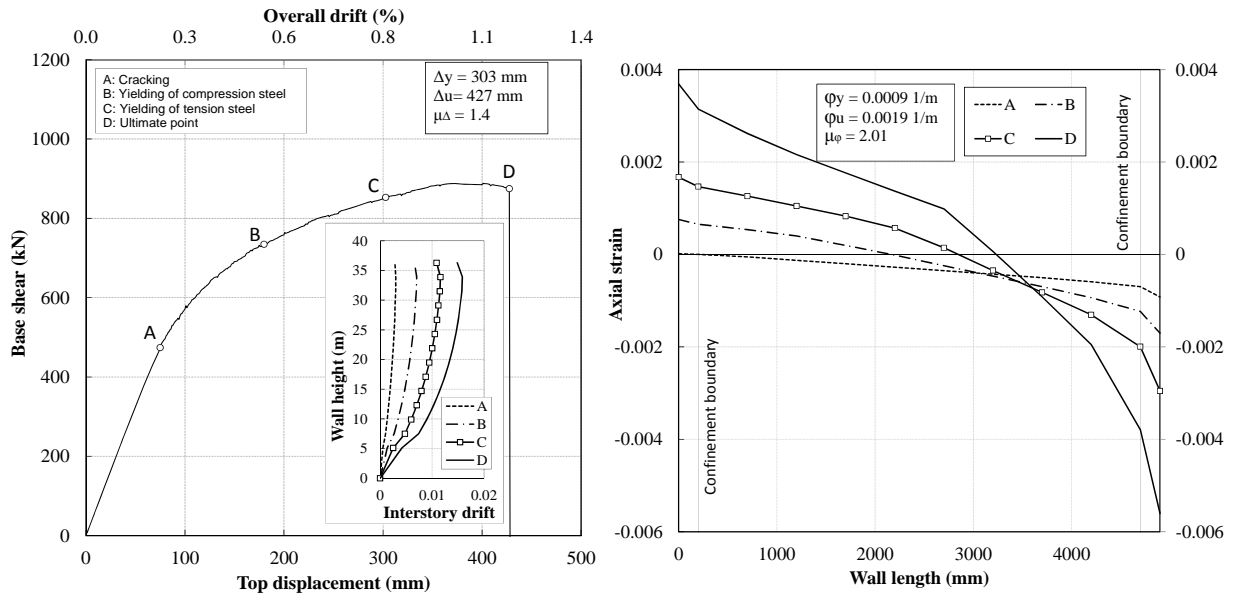


Figure 10. Push-over response of the as-built model

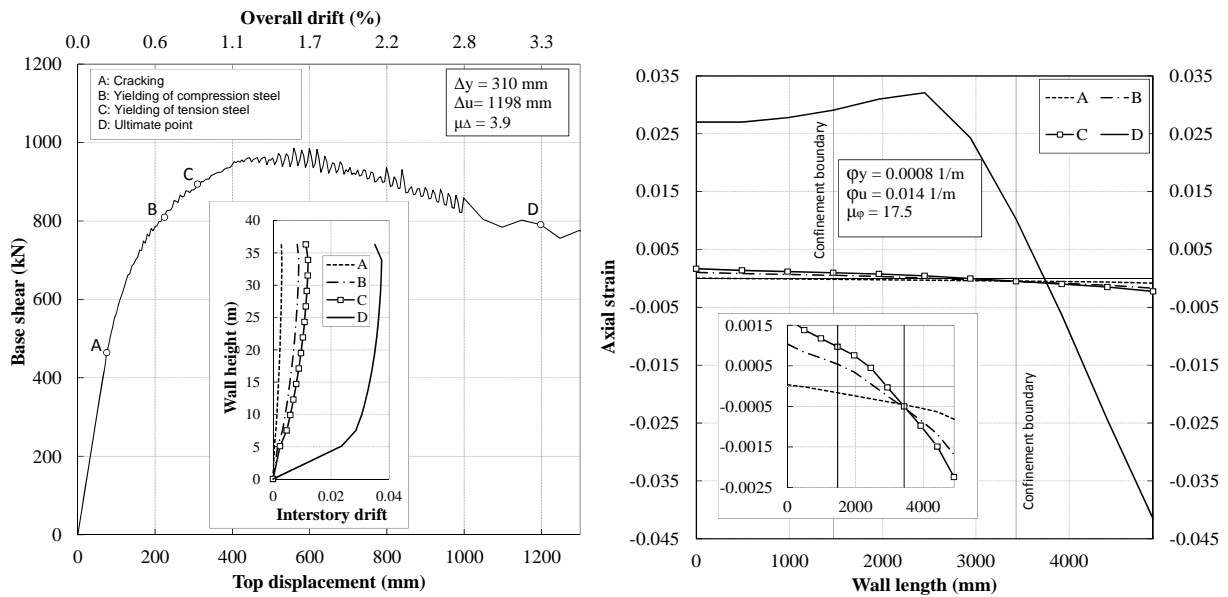


Figure 11. Push-over response of the ACI318-11 model

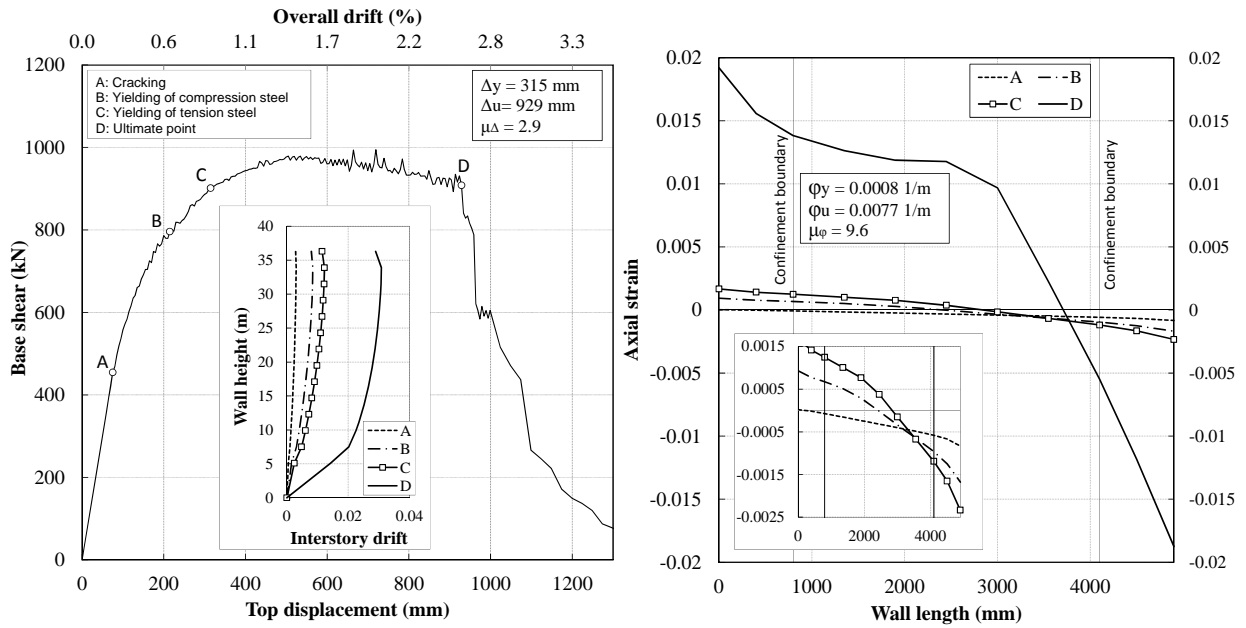


Figure 12. Push-over response of the Eurocode8 model

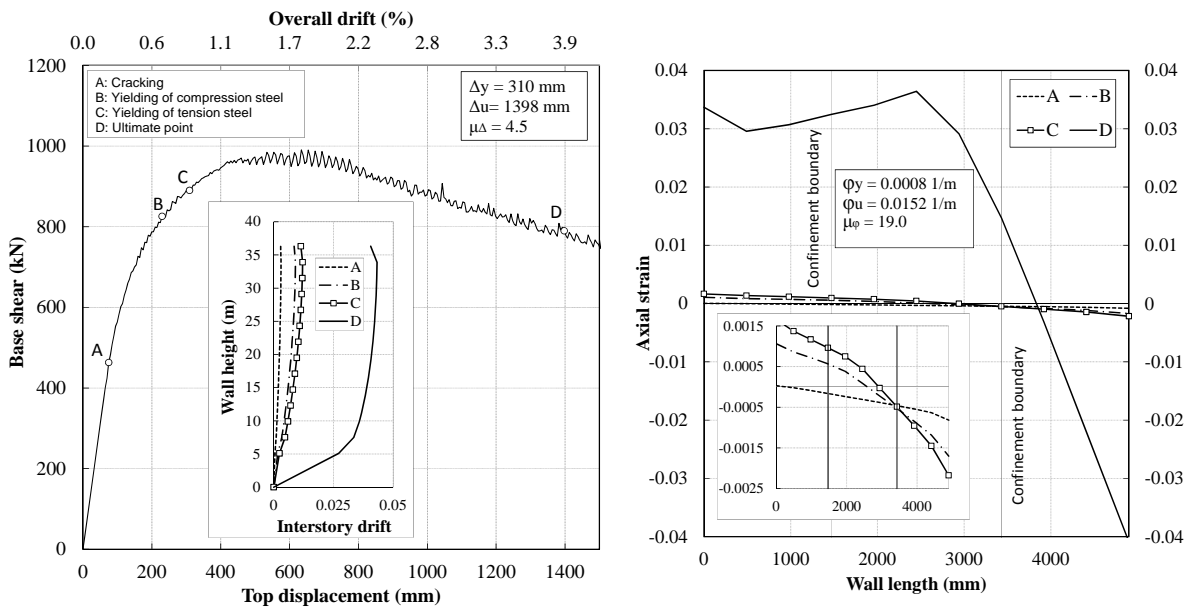


Figure 13. Push-over response of the NZS3101:2006 model

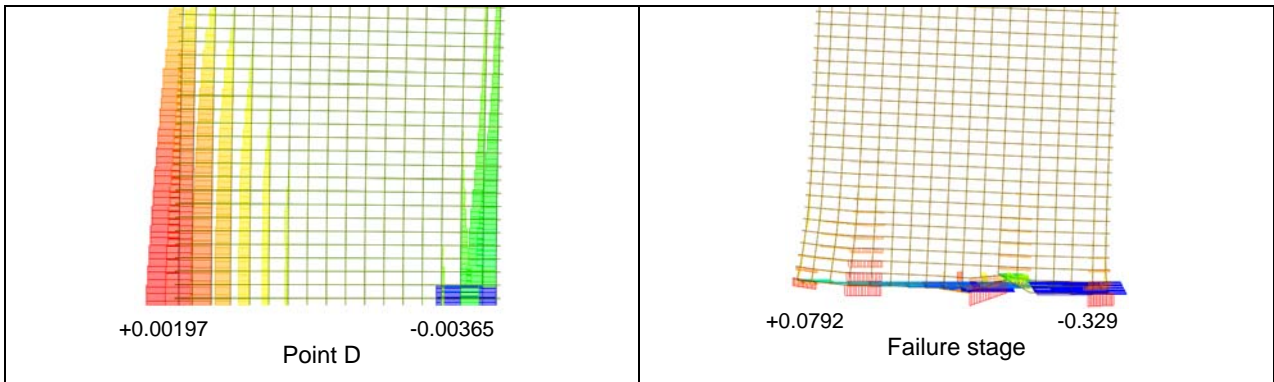


Figure 14. Plastic strain of the reinforcement, As-built

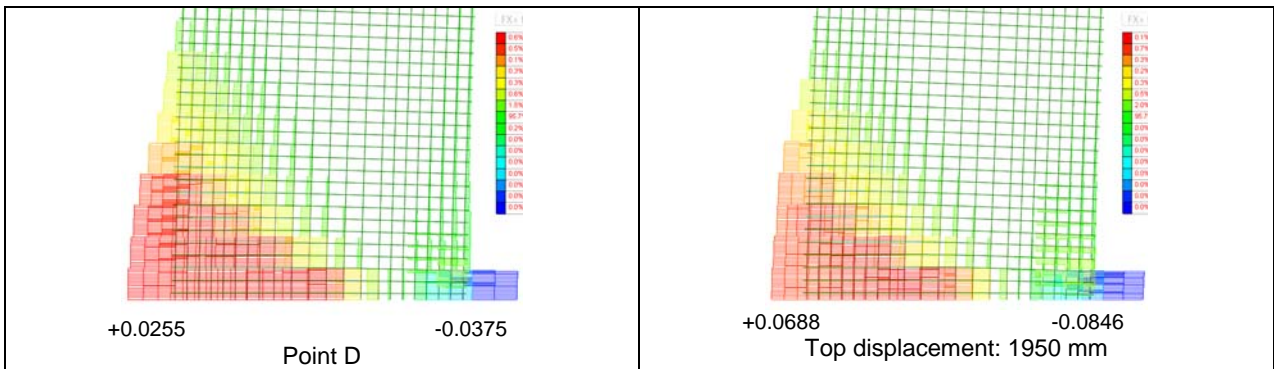


Figure 15. Plastic strain of the reinforcement, ACI318-11

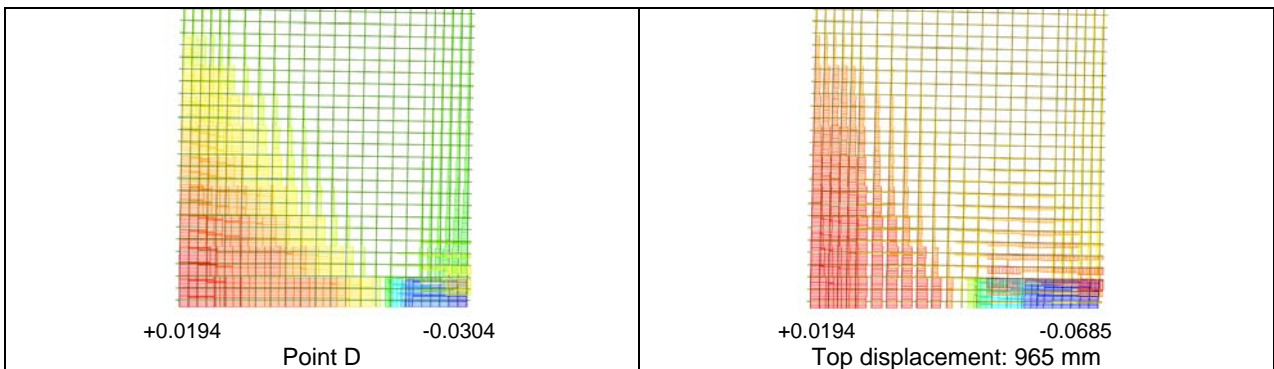


Figure 16. Plastic strain of the reinforcement, Eurocode 8

3.3 Confinement length

In order to investigate the effect of the confinement length on the wall response, the push-over curves of wall models with different confinement lengths were compared. For this purpose, the confinement length of the wall section designed based on ACI318-11 was gradually decreased to reach the confinement length of the As-Built wall (SW1-SW6,

Figure 17). It should be noted that only the confinement length was changed and the boundary and panel reinforcement configuration was kept the same as the ACI318-11 section. Figure 18 compares the response of the wall models SW1 to SW6 as well as the Eurocode8 and as-built models. The confinement length variation is 200mm for all models except between SW2 and SW3 where the variation is only 100mm. Confinement length of the Eurocode8 model is 200mm smaller than SW2 but its ultimate displacement was much smaller. SW3 shows the sensitivity of the degradation point to the confinement length within the region between SW2 and Eurocode8. Based on the detailed investigation of strain profiles and push-over curves of the different models, the critical confinement length appears to be between SW2 and SW3.

Walls with a confinement length greater than the critical value would have a neutral axis positioned within the confined concrete region when the extreme compression strain exceeds the ultimate strain capacity of confined concrete. The effect of confinement length becomes even more significant at larger axial load ratios. As the axial stress increases, the critical compression strain of unconfined concrete is more likely to reach at smaller values of top displacement. This phenomenon was observed in recent earthquakes. According to Wallace (2012), limit should be placed on the axial stress applied to walls. Higher axial stresses in addition to irregular wall cross section shape (eg. T) in Chile earthquake caused concrete compressive strain to reach 0.003 prior to yield of tension steel.

The wall models of ACI318-11 and NZS3101 had such a good confinement that the neutral axis position was within the range of the confinement length at high compression strains and resulted in relatively high level of ductility for these models even after reaching 5.5% average drift. However, as the confinement length decreases, the neutral axis position is more likely to be placed outside the confinement length at critical stages of loading. As for SW4, the failure of the wall occurred at 1.8% average drift. SW6 had the same confinement length as the as-built wall but the transverse reinforcement ratio was the one calculated based on ACI318-11. Thus, the confined concrete model was the same as ACI318-11 (b)

Figure 7(a)) resulting in about 20% increase in displacement ductility compared to the as-built wall.

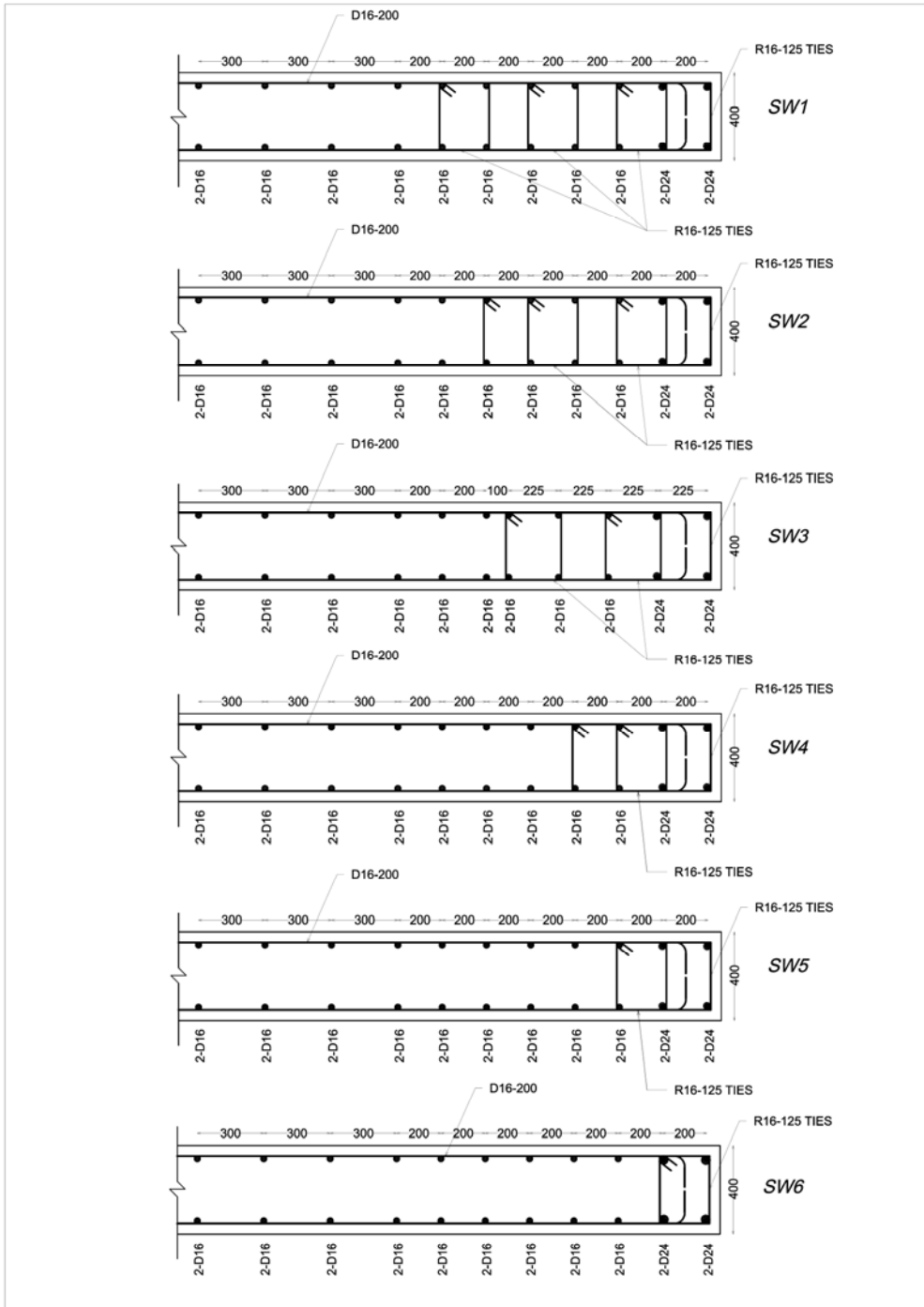


Figure 17. Wall sections with different confinement lengths

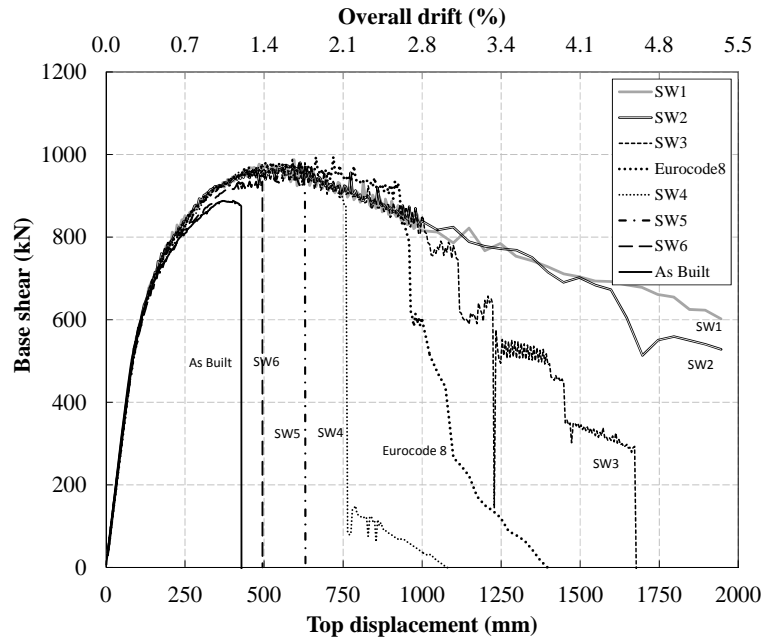


Figure 18. Push-over curves of the wall sections with different confinement lengths

4. CONCLUSIONS

The wall D5-6 of the Grand Chancellor Hotel, which was severely damaged in the February 22, 2011 Christchurch earthquake, was designed based on three seismic design codes; ACI318-11, Eurocode 8 and NZS3101:2006. The four wall models were analyzed at section level (moment-curvature analysis) and member level (push-over analysis) and their responses were compared to understand the effect of different design parameters. The base shear versus top displacement responses of the designed walls were captured using a FEM software. The strain profiles captured at key points of the wall response such as cracking, yielding of tension and compression reinforcement and the ultimate point were used to scrutinize the nonlinear response of the sections designed based on different codes. All the wall sections responded similarly in terms of the points corresponding to cracking, yielding of compression steel and yielding of tension steel. The large amount of axial load applied to the wall resulted in yielding of the compression reinforcement before the tension reinforcement in all models. However, the ultimate point corresponding to the failure of the wall was quite different in the four models.

The wall with the same configuration as the Wall D5-6, denoted as the as-built wall model turned out to be unable to sustain displacement and curvature ductility values greater than 1.4 and 2.0, respectively. Design of the wall based on ACI 318-11 required a considerably greater confinement length with bigger transverse reinforcement ratio and resulted in a section that could sustain displacement and curvature ductilities of 3.9 and 17.5, respectively. The ultimate point of this model was defined as the point corresponding to the 80% of the peak strength as the model did not show any failure up to even 5.5% average drift.

The transverse reinforcement ratio and confinement length of the as-built wall was modified to comply with Eurocode 8, as well. However, the required confinement length based on Eurocode 8 was less than ACI318-11, which caused a brittle failure of the Eurocode8 wall model at about 2.6% overall drift with displacement and curvature ductility values of 2.9 and 9.6, respectively.

The confinement requirements of NZS3101:2006 resulted in a section that was almost the same as ACI318-11 wall model and the only difference was a smaller value of the transverse reinforcement spacing. As a consequence, the displacement and curvature ductility values captured by the NZS3101 section were slightly greater; i.e. 4.5 and 19, respectively.

The curvature values calculated by the strains at extreme fibers captured by the FEM and assuming linear strain profile was in good agreement with the moment-curvature diagram derived from section analysis. However, due to the nonlinearity of the strain profile as well as the P-delta effect that was taken into account in the FEM simulation, the curvature angle of the strain profile was considerably greater.

A parametric study was carried out to further investigate the effect of confinement on the ultimate drift capacity. The confinement length effectively determines the maximum displacement that the wall can undergo without brittle failure of the unconfined concrete. Although providing a good level of confinement using larger amount of hoops with smaller spacing increases the strength and ductility of the wall section, the confinement length plays a key role in the lateral nonlinear in-plane response of RC walls. For example, a section with enough volumetric ratio of transverse reinforcement provided within a smaller length than a critical value is likely to experience an abrupt strength degradation before reaching an acceptable value of displacement as well as curvature ductility.

REFERENCES

- AmericanConcreteInstitute (2011). "Building Code Requirements for Structural Concrete (ACI 318-11) and Commentary (ACI318R-11)." *Farmington Hills, Michigan*.
- CEN, C. E. d. N. (2004). "Eurocode 8: Design of structures for earthquake resistance." *Part 1*, 1998-1991.
- DIANA, T. (2011). Finite Element Analysis User's Manual - Release 9.4.4, TNO DIANA.
- DunningThorntonReport (2011). Report on the Structural Performance of the Hotel Grand Chancellor in the Earthquake of 22 February 2011. Report for the Department of Building & Housing. <http://www.dbh.govt.nz/userfiles/File/Reports/quake-structural-performance-hotel-grand-chancellor.pdf>, Dunning Thornton Consultants Ltd.
- EERI (2011). "The M 6.3 Christchurch, New Zealand, Earthquake of February 22, 2011." *EERI Special Earthquake Report*.
- Elwood, K. J. (2013). "Performance of concrete buildings in the 22 February 2011 Christchurch earthquake and implications for Canadian codes 1." *Canadian Journal of Civil Engineering* **40**(3), 1-18.

- Kam, W. Y., S. Pampanin and K. Elwood (2011). "Seismic performance of reinforced concrete buildings in the 22 February Christchurch (Lyttelton) earthquake." *Bulletin of the New Zealand Society for Earthquake Engineering* **44**(4), 239-278.
- Mander, J., M. N. Priestley and R. Park (1988). "Theoretical stress-strain model for confined concrete." *Journal of structural engineering* **114**(8), 1804-1826.
- NZRC (2012). "Canterbury Earthquakes Royal Commission Reports."
<http://canterbury.royalcommission.govt.nz/Final-Report-Volume-Two-Contents>.
- NZS3101 (2006). NZS 3101:2006 Concrete Structures Standard. Part 1: The Design of Concrete Structures.
- Priestley, M. N. (1996). Seismic design and retrofit of bridges, Wiley-Interscience.
- Telleen, K., J. Maffei, M. Willford, A. Aviram, Y. Huang, D. Kelly and P. Bonelli (2012). Lessons for Concrete Wall design from the 2010 Maule Chile Earthquake. Proceedings of the International Symposium on Engineering Lessons Learned from the 2011, Great East Japan Earthquake.
- TRC (2011). XTRACT, Imbsen Software Systems, 9912 Business Park Drive, Suite 130, Sacramento, CA95827.
- Wallace, J. (2012). "Behavior, design, and modeling of structural walls and coupling beams — Lessons from recent laboratory tests and earthquakes." *International Journal of Concrete Structures and Materials* **6**(1), 3-18.